Low-temperature conduction in germanium with disorder caused by extended defects

1993 J. Phys.: Condens. Matter 5 2351

(http://iopscience.iop.org/0953-8984/5/15/008)

J. Phys.: Condens. Matter 5 (1993) 2351–2376. Printed in the UK

Low-temperature conduction in germanium with disorder caused by extended defects

M L Kozhukh†

A F Ioffe Institute of Physics and Technology, 194021, St Petersburg, Russia

Received 28 April 1992, in final form 9 December 1992

Abstract. Investigations were carried out on low-temperature conductivity in the defect band of germanium formed due to the presence of large concentrations of extended defects introduced during high-temperature plastic deformation or irradiation with large integrated fluxes of high-energy neutrons and protons. It has been demonstrated that at relatively low concentrations of dislocations and low temperatures the electrical conductivity in the defect band occurs by hopping. At higher concentrations of dislocations the metal–insulator transition (MIT) takes place in the system of dislocations, the conductivity near the MIT showing a power-law variation, $\sigma(T) \sim T^x$, with $x \leqslant 1$ in the range 30 to 3×10^{-2} K. It has also been shown that the dislocation conductivity has a quasi-two-dimensional character. The dynamics of the Coulomb gap variations was studied near the MIT in Ge with a high concentration of radiation defects. The experimental data presented show that Ge with a high concentration of dislocations can be used for simulating some physical phenomena in amorphous and vitreous semiconductors.

1. Introduction

A large number of original works and reviews have been published that deal with dislocations and radiation defects and their influence on electrophysical properties of semiconductors. However, these are mostly concerned with the influence on the band motion of charge carriers of low densities of defects at temperatures where the charge transport is due to free carriers, i.e. in conditions when localization of the carriers does not occur and an aperiodic potential due to dislocations affects only an insignificant part of the carrier path. In a few works [1,2] the influence of irradiation with rather low fluxes of fast neutrons on low-temperature conduction in doped n-type germanium was studied and conduction due to dislocations in plastically deformed germanium at low temperatures observed [3]. However, detailed experimental studies of carrier transport via localized states in semiconductors with high density of dislocations or radiation defects have not yet been undertaken. Besides, the random character of the distribution of the electric field acting on the charge carriers in the widely applied amorphous, liquid and vitreous semiconductors makes difficult the mathematical description of such systems and understanding the nature of the phenomena observed.

In modelling these disordered systems, investigations of more simple systems behaving in a similar way, for example, crystalline semiconductors with a large density of dangling bonds, could have been of use. Dangling bonds can be produced in a crystal by introducing

† Present address: Department of Electrical Engineering and Applied Physics, Case Western Reserve University, Cleveland, OH, USA.

0953-8984/93/152351+26$07.50

in it dislocations or radiation defects. In the present paper we report results of experimental investigations of galvanomagnetic phenomena at low temperature in highly plastically deformed single-crystalline germanium and silicon and polycrystalline germanium as well as in germanium irradiated with large fluxes of fast reactor neutrons and protons of energy $E = 1$ GeV. Ge and Si are considered as crystals with a disorder controlled in a wide range by plastic deformation, irradiation with high-energy radiation, annealing and initial doping.

2. Low-temperature electrical conductivity of plastically deformed germanium

Studies of carrier transport in the DC regime at liquid-helium temperatures in plastically deformed germanium (PDG) for dopant concentrations $N \leqslant 10^{14}$ cm^{-3} is possible only at high densities of dislocations, sufficient for the formation of a defect band (in analogy with an impurity-doped material). As a means of producing considerable structural disorder and of introducing dislocations in germanium, plastic deformation caused by uniaxial compression along the [1 1 1] axis at temperatures 800–820 °C was used [4]. The choice of such a high temperature is explained by the necessity of obtaining high deformations (high density of dislocations and other extended defects); besides, at high temperatures, point defects are annealed and the system of dislocations formed possesses long-term stability. The technique of sample preparation is described elsewhere [5, 6]. Figure 1 shows the dependence of the free hole concentration $p = 1/eR_H$ (e being the electron charge and R_H the Hall constant) at 300 and 77 K on plastic deformation D for low-doped n-Ge with $N = 3 \times 10^{13}$ cm^{-3}. It is seen that the hole concentration rises with increasing deformation, indicating an increase in the number of dislocations introduced. For germanium the maximum value of D that could be achieved using the technique described above was $\approx 50\%$ (for silicon 70%). At higher deformations Ge samples were destroyed. Dislocation patterns produced at such high D values are very difficult to interpret.

We are not interested in its details but rather in disordered systems in general, in which an aperiodic potential of varying magnitude due to extended defects affects carrier transport at low temperatures. As seen from figure 1, the hole concentration at $T = 300$ K and $D > 20\%$ exceeds 10^{15} cm^{-3}, a level at which impurity hopping conduction sets in in impurity-doped p-Ge [7]. However, while dopants are distributed nearly uniformly throughout the bulk of a semiconductor, dislocations in PDG occupy but a small fraction of the total volume. Therefore, at rather low average carrier concentration their local density in PDG can be higher. A tendency to saturation apparent in figure 1 warrants a suggestion that heavily doped n-Ge with an impurity concentration of about 10^{17} cm^{-3} cannot be converted to p-type throughout its volume, though local conversion can take place. We shall see below that this is indeed so. Captured electrons do not satisfy all dangling bonds on dislocations because of Coulomb repulsion by captured electrons, so the existence of unfilled positions at dislocations can be compared to the introduction of a compensating impurity into a doped semiconductor.

Simultaneously, because of anisotropic distribution of dislocations in the Ge crystal, free carriers possess a corresponding anisotropy of the Hall mobility. Figure 2 shows the variation of the Hall mobility $\mu = R_H/\rho$ at 77 K for samples with long axes both along the uniaxial stress direction, i.e. along [1 1 1] (denoted $\parallel$ in the figure), and perpendicular to the stress direction (denoted $\perp$). The presence of dislocations causes additional scattering and, evidently, lowers the mobility in all crystallographic directions, while the anisotropy is due to the non-uniform distribution of dislocations in PDG. Figure 3 shows the temperature dependences of the resistivity and R_H for samples ($\perp$) with 20 and 30% deformations. It

is seen that at essentially the same temperature T_0 there is observed a maximum on the $\lg[R_H(1/T)]$ curve and an inflection on the $\lg[\rho(1/T)]$ curve. An analogous form has a low-temperature electrical conductivity due to impurities at concentrations corresponding to hopping conduction in the impurity band [7, 8]. On lowering the temperature the carriers are 'frozen out' of the conduction band (an n-type semiconductor is assumed). A corresponding exponential rise of the Hall coefficient R_H is observed.

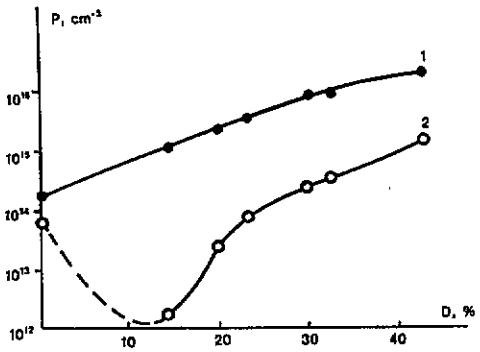

Figure 1. Dependences of the hole concentration on plastic deformation value at $T = 300$ K (1) and 77 K (2).

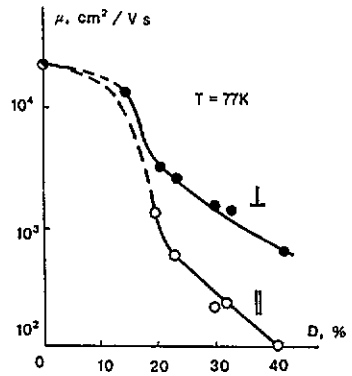

Figure 2. Dependences of the mobility at 77 K on plastic deformation value in directions parallel (∥) and perpendicular (⊥) to the deformation axis.

It is seen in figure 3 that, for $T > T_0$, $\rho(T)$ curves have an exponential character with activation energies E_1 equal to 70 and 40 meV for samples with $D = 20$ and 30%, respectively. Note that with increasing dislocation density (at higher deformations) E_1 decreases, also in analogy with impurity-doped semiconductors. As with the conductivity of impurity-doped germanium, it may be supposed that in the range $T > T_0$ conduction is due to free holes thermally ejected from the levels produced by dislocations into the valence band, whereas at $T < T_0$ conduction via dislocations dominates because other sources of charge carriers in Ge with $N = 3 \times 10^{13}$ cm^{-3} are absent. Shown in figure 4 on a log–log scale are plots of $\rho(T)$ for samples of both types. Strong anisotropy of the conductivity is apparent. Even for a sample with $D = 43\%$ for which the anisotropy is minimal the conductivity ratio in both directions at 4.2 K reaches $\approx 10^4$. An effect of this magnitude was observed earlier at $T = 300$ K in plastically deformed ZnS [9] and explained by a 'one-dimensional' character of the dislocation band. In our case the anisotropy arises from different temperature dependences of the conductivity via dislocations in different crystallographic directions: the electrical conductivity of PDG in the (1 1 1) plane is considerably higher than along the [1 1 1] axis.

The difference is so great that the conductivity can be considered as a quasi-2D one and the material as being 'layered' with respect to its electrical properties as a result of plastic deformation. The formation of 'conducting' layers in the (1 1 1) planes is, possibly, due to the fact that in diamond-like semiconductors plastic shear under stress occurs just in the (1 1 1) planes, which thus contain the largest density of structural defects (dislocations) acting as localization centres in PDG. As the value of deformation (disorder) increases, so does the 'interaction' between the high-conductivity layers and the anisotropy becomes less. At high temperatures ($T \geqslant 100$ K) where the band conduction dominates, the anisotropy disappears. Conductivity curves for samples with $D = 14$, 20 and 23% if plotted on a

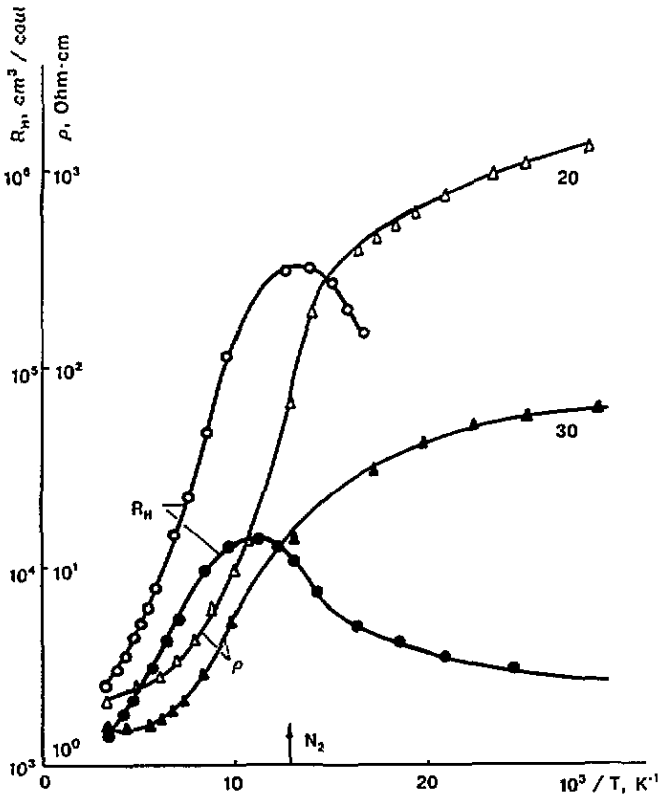

Figure 3. Temperature dependences of the resistivity and Hall constant for samples with $D = 20$ and 30%.

log–log scale have the appearance of exponential dependences ('concave') and can be fitted with an expression $\sigma = \sigma_0 \exp[-(T_0/T)^y]$, where σ_0 and T_0 are constants and $y = 0.7$–0.8 (determined by differentiating the curves), while in samples with D of 30 and 43% at liquid-helium temperatures a power-law dependence is observed, $\sigma \sim T^x$, where $x = 1.0$ or 0.5 for samples with $D = 30$ and 43%, respectively. Figure 5 shows the dependence of ρ on D at a fixed temperature (20 K). It is seen that $\sigma = \rho^{-1}$ rises exponentially in a D range from 15 to 30% and then much more slowly.

A consideration of the behaviour of PDG with $D \geqslant 30\%$ will be given below. The data relating to PDG with $D < 30\%$ may be summed up as follows: (i) the resistivity depends on a deformation value (dislocation density) exponentially; (ii) the temperature dependences of the Hall constant $R_H(1/T)$ and $\rho(1/T)$ feature a maximum and an inflection, respectively, at about the same temperature; (iii) in the low-temperature range the Hall voltage is unmeasurable; (iv) the temperature dependence of the conductivity is of the activation type; and (v) current–voltage characteristics contain superlinear portions [5]. Thus, it may be concluded that the low-temperature conductivity of lightly doped PDG at relatively 'weak' deformations ($14\% \leqslant D < 30\%$ for the technique of sample preparation employed) is of the hopping type with variable activation energy and occurs by hops of localized carriers between dislocations.

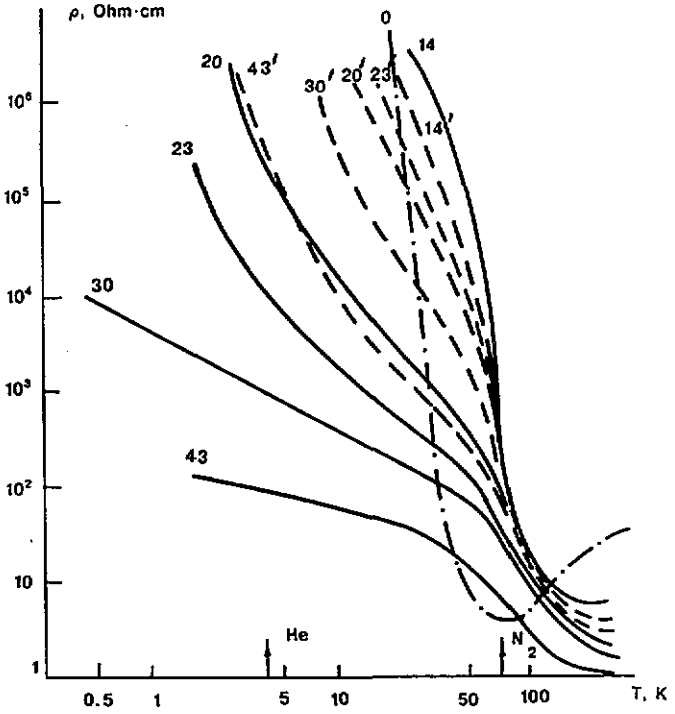

Figure 4. Temperature dependences of the resistivity along the deformation axis (broken curves) and in a direction perpendicular to the deformation axis (full curves). Figures by the curves give deformation values.

3. Interaction between impurities and dislocations in doped germanium

In this section the properties of PDG containing shallow impurities (Sb, Ga) are considered. The impurity concentration in the starting germanium was chosen such that at liquid-helium temperatures conduction occurred in the impurity band. Two versions are considered:

(i) Conduction in the starting material is by hopping in the 'E_3 region'; this version corresponds to a concentration of antimony in germanium of $N = 2.5 \times 10^{16}$ cm^{-3}.

(ii) Conduction in the starting material is metallic, i.e. the dopant concentration exceeds the critical one n_c for the metal–insulator transition (MIT); the starting impurity concentration in Ge in this case is $N = 4.9 \times 10^{17}$ cm^{-3}.

3.1. Version (i)

Figure 6 shows the variation of the free-carrier concentration and Hall mobility μ in the samples at $T = 300$ and 77 K with deformation D. As D is increased, n and μ are seen to decrease and ultimately a conversion to p-type takes place. These results agree with the assumption that dislocations in n-Ge behave generally as acceptors and cause compensation and additional scattering [10]. Figure 7 gives the variation of the conductivity with temperature for a number of samples with different values of deformation. Curve 0 is measured on a reference sample subjected to the same thermal treatment but free of deformations. In the low-temperature range this sample exhibits hopping conduction (HC)

involving antimony atoms with a constant activation energy E_3: $\rho(T) = \rho_3 \exp(E_3/kT)$. The parameter ρ_3 is determined by an overlap integral [11] and varies exponentially with mean distance R between impurity atoms ($R \sim N^{-1/3}$). E_3 is the energy from the Fermi level to the maximum in the density of states and is a measure of the impurity bandwidth. It follows from figure 7 that until the conversion point is reached the hopping conductivity falls with rising D, while both ρ_3 and E_3 increase. This is contrary to the familiar mechanism of compensation on account of acceptor levels produced by plastic deformation.

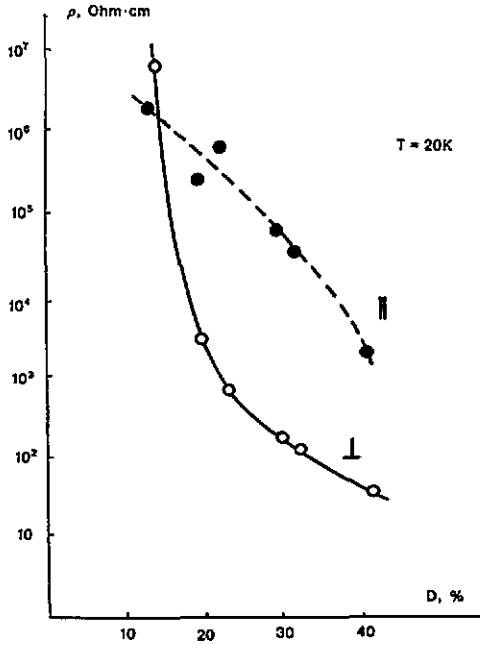

Figure 5. Dependence of the resistivity on plastic deformation at $T = 20$ K.

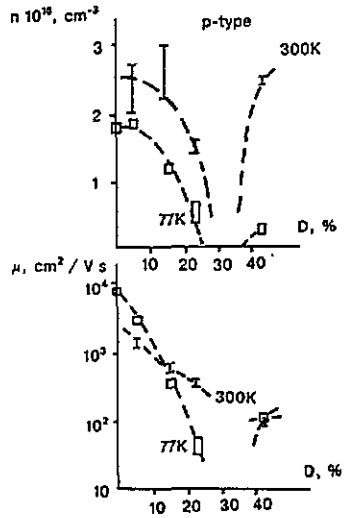

Figure 6. Dependences of the concentration n and mobility μ of charge carriers on deformation value in n-Ge.

Indeed, with increasing degree of compensation K the hopping conductivity initially increases due to falling E_3 and increasing number of positions available for carrier jumps, reaches a maximum at $K = 0.5$ and only then begins to drop, whereas experiments show that in germanium with deformations 5 and 15% for which Hall data give $K < 0.5$ the hopping conduction is noticeably reduced. An increase in E_3 can be evidence of impurity band broadening because of non-uniform lattice deformation caused by a large number of introduced dislocations. The main factor, however, is an increase in ρ_3 indicated by the intersection on the ordinate axis. This quantity depends on the parameter R/a, where a is the Bohr radius of an electron localized on the donor. The increasing ρ_3 and the observed anisotropy of the hopping conduction for D values of 15 and 23% can possibly be explained by the presence in PDG of a residual strain. It is known [12] that for maximally effective uniaxial elastic deformation along the [1 1 1] axis the wavefunction of a donor in n-Ge becomes highly anisotropic and overlapping of the wavefunctions in the case when the impurity is antimony becomes less. However, as shown in [12], even in the case of 'extreme' elastic deformations along the [1 1 1] direction the ρ_3 value in n-Ge with the same

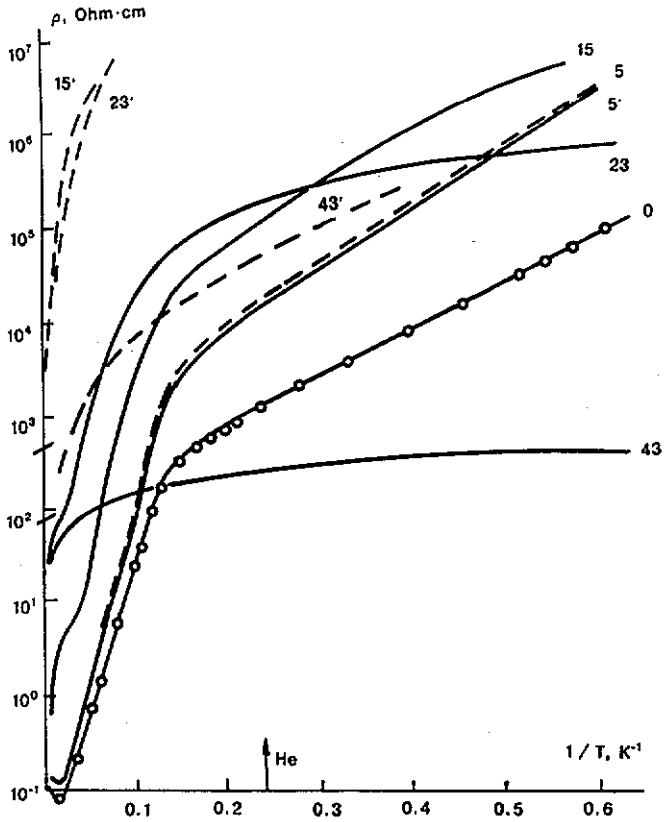

Figure 7. Temperature dependences of the resistivity for n-Ge with an initial concentration $N(\mathrm{Sb}) = 2.5 \times 10^{16}$ cm^{-3}. Figures by the curves give deformation values; primed figures relate to parallel ($j \parallel$ [1 1 1]) and unprimed to perpendicular ($j \perp$ [1 1 1]) configurations; the current flow is in the (1 1 1) plane.

concentration of antimony does not exceed 10^4 Ω cm, which is less than in PDG, especially when the current direction coincides with the deformation axis (samples denoted by ∥).

Besides, the anisotropy of hopping conduction, as shown in [13], should not exceed the anisotropy of the wavefunction proper, which in Ge is around 4–5, again a contradiction with the experimentally observed anisotropy of the conductivity (more than 10^2–10^3, as seen in figure 7). Thus, we have to conclude that plastic deformation causes an increase in ρ_3, i.e. the number of impurities taking part in hopping conduction is reduced, the reduction being different in different directions. We believe this to be caused by 'attraction' of impurities by dislocations in the deformation process. It might, of course, be supposed that the spatial distribution of impurities does not change but, instead, a fraction of impurities, found in the proximity of dislocations, microcracks and other defects as a result of plastic deformation, have their energy levels considerably altered (for example, pushed up into the conduction band) so that localization of electrons by these impurities is no longer possible. The net result would have been a reduction in the number of impurities taking part in the hopping conduction. This, however, would have reduced the free-electron concentration at high temperatures (300 K), when the electrons are released from impurities into the conduction band. The experimental picture is different; e.g. in a sample with $D = 5\%$ an increase in ρ_3 corresponded to an electron concentration n lower by a factor of 1.8, whereas the measured

concentration was essentially unchanged.

It has to be assumed that attraction of impurities by dislocations is consistent with this experimental observation, because the hopping conduction is governed by regions where the impurity is rarified. Note that, if the dislocations were to form a continuous network throughout the sample, from one contact to another, then the reduction of the hopping conductivity would not have been observed because of conduction via regions around dislocations rich in impurities. We conclude, therefore, that what is termed here low-temperature conduction via dislocations in lightly doped (intrinsic) plastically deformed germanium occurs by carrier jumps between dislocations and not as their movement along the dislocation core. Formation around dislocations of an 'atmosphere' of impurities is a known phenomenon [10]. The dislocation density at which rarification of impurities takes place is estimated at 10^9–10^{10} cm^{-2}, corresponding to an average distance l_0 between dislocations of $l_0 \approx 10^{-5}$ cm. Impurity atoms (in our case Sb) accumulate at dislocations during high-temperature plastic deformation if $l_D > l_0$, where $l_D = (Dt)^{1/2}$ is the diffusion length, D the diffusion coefficient and t the process duration.

The diffusion coefficient of Sb at $T = 800\,^{\circ}$C equals $D = 2.0 \times 10^{-11}$ cm^2 s^{-1} [14], so the diffusion length during plastic deformation is $l_D \approx 10^{-4}$ cm, i.e. indeed, $l_D > l_0$. In investigations of low-temperature conductivity in PDG the anisotropy of hopping conduction via dislocations was observed. It is seen from figure 7 that the HC via impurities in samples with $D = 15$ and 23% also has a two-dimensional character. Taking into account that geometry and conditions during plastic deformation of doped germanium were identical, this fact may be considered as one more piece of evidence that impurities are attracted by dislocations. The temperature dependence of the conductivity in the most strongly deformed specimen with $D = 43\%$, which has been converted to p-type, is close to that for intrinsic germanium, this being true for both crystallographic directions in question. It may thus be concluded that in this material charge transport takes place via dislocations, the presence of the impurity 'atmospheres' around dislocations not affecting the conductivity in a significant way [15].

3.2. Version (ii)

Figure 8 shows the $\rho(T)$ dependence for plastically deformed n-Ge doped with antimony to such a level that the conductivities in the starting and reference specimens were of metallic type (temperature independent) but not too far from the point where the MIT occurs. In our samples N was 4.9×10^{17} cm^{-3}. Particular features of the MIT in lightly and medium-doped germanium with high degree of structural disorder will be discussed below. Here it is to be noted only that in heavily doped material plastic deformation lowers the impurity conduction, makes it anisotropic and temperature-dependent, while causing but insignificant changes in the free-carrier concentration at $T = 300$ K (table 1). So, in this case the experimental data [16] also give evidence of the impurities being rarified in the bulk semiconductor. To test the hypothesis that the mobility of Sb atoms during high-temperature plastic deformation affects the low-temperature conductivity of PDG, experiments were conducted on p-type germanium containing relatively low-mobility Ga atoms (coefficient of diffusion $D = 10^{-13}$ cm^2 s^{-1} at $T = 800\,^{\circ}$C [14]). The gallium content, $N_{Ga} = 8 \times 10^{15}$ cm^{-3}, was chosen such that the low-temperature conduction occurred via impurities. Figure 9 gives the temperature variation of the conductivity in a reference sample and in samples deformed by 33%. It is seen that, as a result of plastic deformation, the conductivity at liquid-nitrogen temperatures, which is dominated by scattering of the free holes in the valence band, became lower and anisotropic. This can be explained as due to a mechanism of anisotropic carrier scattering by dislocations in the region of band conduction, the anisotropy arising from different

concentrations of scatterers along the [1 1 1] axis and in the (1 1 1) plane. On the other hand, at liquid-helium temperatures, where conduction is due to hopping of holes localized at acceptor impurities and depends exponentially on the overlap factor R/a, no appreciable changes in the magnitude of conductivity or the value of the pre-exponential factor ρ_3 are observed. This indicates the absence of changes of the mean distance between acceptor impurity atoms R and the Bohr radius in germanium having a high density of dislocations.

Table 1.

D (%)	0	18	25	28
$N \times 10^{-17}$ (cm^{-3}) at $T = 300$ K	4.9	4.0	3.5	3.2

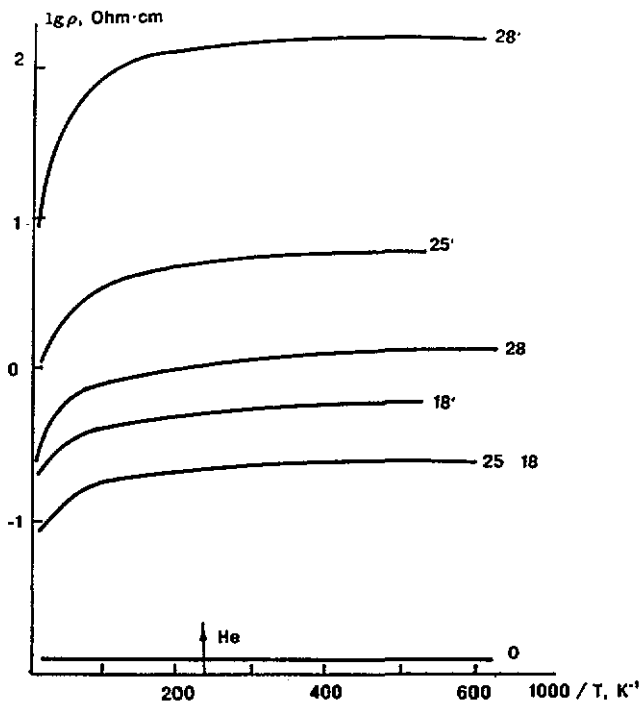

Figure 8. Temperature dependences of the resistivity for n-Ge with an initial impurity concentration $N(\mathrm{Sb}) = 4.9 \times 10^{17}$ cm^{-3}. Figures by the curves give deformation values; primed figures relate to parallel ($j \parallel [1\,1\,1]$) and unprimed to perpendicular ($j \perp [1\,1\,1]$) configurations, respectively; the current flow is in the (1 1 1) plane.

The observation that impurity HP is unaffected by a potential due to the dislocations introduced by plastic deformation in p-Ge makes one wonder whether this would be so in any situation, including the case of a large concentration of defects at the boundary between mosaic blocks (for relatively large intergrowth angles), or whether the reason is the relatively low density of defects at the grain boundaries in a textured polycrystal with blocks only slightly disoriented such as in PDG (PDG structure will be considered below). An experimental test of the above considerations was carried out on polycrystalline

germanium in which mosaic blocks turned round up to 360°. To avoid precipitation of the impurity at the grain boundaries observed for doping in the melt, the shallow impurity was introduced with the use of transmutations occurring in nuclear reactions of ^{70}Ge, ^{74}Ge and ^{76}Ge with slow neutrons under irradiation in a uranium–graphite power reactor RBMK-1000 [17, 18]. Two groups of samples of polycrystalline float-zone-purified germanium with impurity concentration $< 10^{13}$ cm^{-3} were irradiated in integrated fluxes $\Phi \approx 4 \times 10^{17}$ and 2.5×10^{17} neutrons cm^{-2} (irradiation times 50 and 30 min, respectively). Following deactivation of the surface and after a time sufficient for the radiation from the bulk to drop to an admissible level, complete annealing of the radiation defects was performed at 450 °C (24 h). Figure 10 shows $\rho(T)$ curves for two neutron-doped samples and, for comparison, curves for two monocrystalline neutron-doped samples taken from [7]. It is seen from the figure that for the two values of the doping impurity concentration the magnitude and behaviour of the electrical conductivity in monocrystalline and polycrystalline germanium at high temperatures (region of E_1 conduction) coincide, whereas values of the low-temperature conductivity in the impurity band for the two materials differ, the activation energy in the polycrystalline germanium being noticeably less for both concentrations of the doping impurity. At the same time, the neutron-doped polycrystalline material, though possessing highly uniform impurity distribution, exhibits considerable anisotropy of the hopping conductivity for two arbitrarily chosen directions perpendicular to each other. Because in undoped polycrystalline germanium the low-temperature conductivity along grain boundaries is practically zero (figure 10(*a*), curve 1′), these experimental data indicate that extended acceptor centres forming at the grain boundaries and containing a high density of defects enhance jumps of the carriers in the impurity band due to shallow acceptors and significantly reduce the activation energy for HP.

4. Metal–insulator transition in lightly doped plastically deformed germanium

As can be seen in figure 4, the temperature dependences of conductivity in PDG with $D > 30\%$ and $D < 30\%$ differ in principle: in the former it is a power-law dependence unusual for semiconductors, while in the latter it is the usual exponential dependence with varying activation energy. A question arises of whether or not the power-law curve might in fact be an extension of the 'smooth' exponential, difficult to recognize because of the narrowness of the temperature range investigated. It is known that in doped semiconductors the metal-insulator transition takes place as the impurity concentration is increased, the conductivity on the metallic side being practically temperature independent and, on the insulator side, exponential up to the transition. In the ultra-low-temperature range the activation energy of conductivity is not a constant but decreases with temperature, in accord with the Mott mechanism of conduction with variable hopping length [19].

Nonetheless, the activation energy decreases more slowly than the energy equivalent of temperature, so that the exponential character of conduction persists down to 0.05 K [20] and is distinctly seen in log plots of $\rho(T)$, the curves having a typical 'concave' form. Figure 11 shows $\rho(T)$ curves at ultra-low temperatures [21] for (intrinsic) PDG with $D = 30$ and 43% (curves 1 and 2), n-Ge doped with Sb to 2.5×10^{16} cm^{-3} and having $D = 43\%$ (curve 3), as well as the curves (a, b, c) for neutron-doped germanium [20]. The measurements were performed in a ^{3}He–^{4}He dilution cryostat. It is seen that down to 0.03–0.04 K the transition to activated conduction does not occur, i.e. the region of power-law temperature dependence of the conductivity extends from 30 to 0.03 K. To this it should be added that the temperature dependence of the carrier concentration (Hall effect)

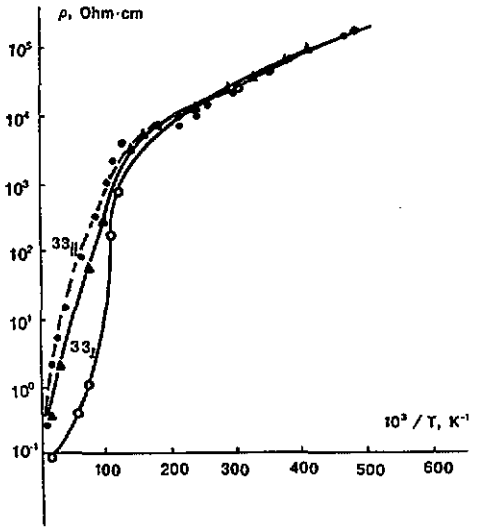

Figure 9. Temperature dependences of the resistivity for the starting sample of p-Ge with an initial gallium concentration of 8×10^{15} cm^{-3} and for two samples deformed by 33%, with j in the (1 1 1) plane ($33_{\perp}$) or along the [1 1 1] axis ($33_{\parallel}$).

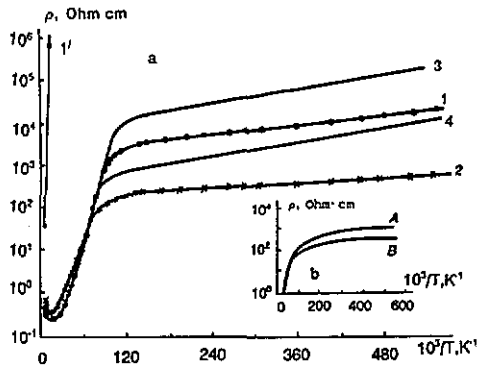

Figure 10. Temperature dependences of the resistivity: (*a*) 1', starting germanium sample with $N_A - N_D < 10^{13}$ cm^{-3}; 1, 2, neutron-doped polycrystalline germanium with $N = 4.2 \times 10^{15}$ and 7.4×10^{15} cm^{-3}, respectively; 3, 4, samples of neutron-doped single-crystal germanium [7] with $N_A - N_D = 3.6 \times 10^{15}$ cm^{-3} and 7.2×10^{15} cm^{-3}, respectively; (*b*) $\rho(T)$ for a sample of neutron-doped polycrystalline germanium with $N_A - N_D = 7.4 \times 10^{15}$ cm^{-3}, for two arbitrarily chosen mutually perpendicular directions (A, B).

for lightly doped germanium with $D = 43\%$ in the range 4.2–1.7 K is quite weak (figure 12), which is possibly evidence not of the change in carrier concentration in the dislocation band (in this case the concentration dependence would have been exponential in character) but of the mobility variation with temperature. In the range of dislocation band conduction (for intrinsic Ge with $D \geqslant 30\%$ [5,21]) the following has been observed: a transition to conduction that is not activation type, the Hall effect is measurable, the temperature dependence of the Hall constant being non-exponential and the conductivity exhibiting no dependence on frequency.

This leads to the conclusion that the low-temperature conduction is due to delocalized carriers in the dislocation band and is metallic in character. All these phenomena are typical also for conduction via impurities on the metallic side of the transition. Apart from strong anisotropy of the conductivity, arising from the distribution of dislocations peculiar to crystals with the diamond structure, the difference consists in that the impurity band conduction on the metallic side is essentially temperature independent, whereas in the case of conduction in the dislocation band the temperature dependence obeys the power law. It should be remarked though that a power-law temperature dependence of the conductivity as well as a temperature-independent Hall constant were observed [22] in n-Ge on the metallic side of the MIT produced by uniaxial elastic strain. This indicates that the power-law temperature dependence of conductivity is limited to a narrow concentration range near the MIT in impurity-doped germanium and can exist in a much wider range in dislocation-doped germanium. The observation that x in $\sigma(T) \sim T^x$ decreased with increasing D suggested that the conductivity might ultimately become temperature independent, which has been confirmed in [23,24]. It may thus be stated that near the MIT the temperature dependence

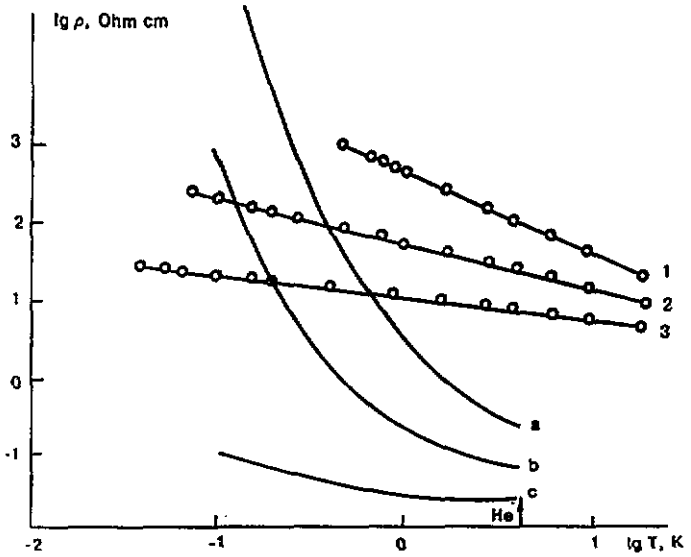

Figure 11. Temperature dependences of the resistivity in the range of ultra-low temperatures: 1, 2, Ge ($N = 3 \times 10^{13}$ cm^{-3}), deformation value $D = 30$ and 43%, respectively; 3, Ge(Sb), $N = 2.5 \times 10^{16}$ cm^{-3}, deformation value $D = 43\%$; a, b, c, curves 2, 3, 4 from [20].

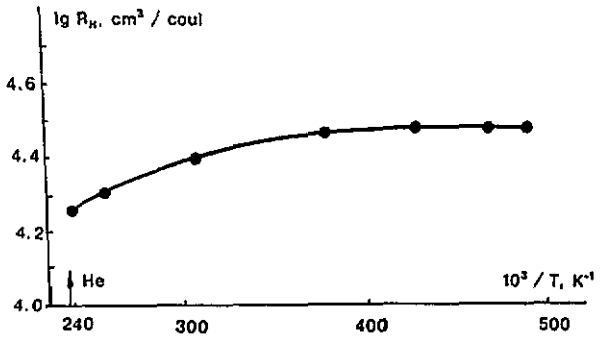

Figure 12. Temperature dependence of the Hall constant R_H for a sample of low-doped germanium ($N = 3 \times 10^{13}$ cm^{-3}), deformation value $D = 43\%$, $H = 0.6$ T.

of the conductivity has power-law but not exponential character.

5. Metal–insulator transition in disordered heavily doped germanium

Much interest is caused by the situation when structural disorder has been created in single-crystal n-Ge doped previously in such a manner that it is found just on the metallic side of the MIT [2]. In this case introduction of acceptor centres in sufficient quantities should result in activated conduction in the temperature range 300–30 K, then followed by an exponential or power-law conduction, depending on the relative amounts of impurities and dislocations. Indeed, as seen from figure 13, cessation of metallic conduction and transition to semiconductor conduction occurs in n-Ge with $N(\mathrm{Sb}) = 2 \times 10^{17}$ cm^{-3} under plastic deformation or in n-Ge with $N = 7 \times 10^{17}$ cm^{-3} as a result of irradiation with 1 GeV protons (integrated flux $\Phi \approx 2 \times 10^{17}$ cm^{-2}). In samples deformed by 13 and 25%, variable-range hopping or Mott-type conduction is observed, described by the formula $\sigma(T) \approx$

$\exp[-(T_0'/T)^{1/4}]$, T_0' being a constant, whereas in the n-Ge sample deformed by 46%, power-law conduction is observed. All the samples after plastic deformation or irradiation with protons remained n-type. Though retaining n-type conductivity, the conductivity in germanium deformed by 46% shows a power-law dependence on temperature, $\sigma(T) \sim T^x$, where $x < 1.0$.

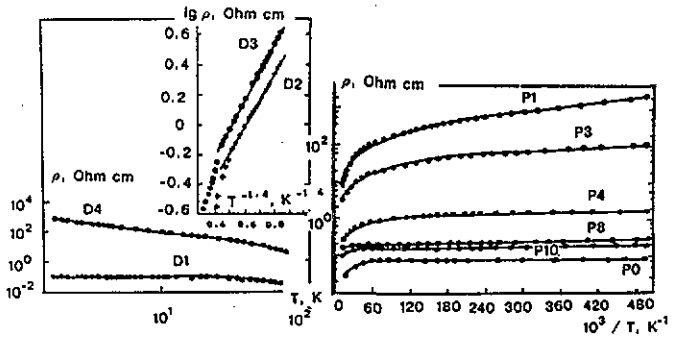

Figure 13. (*a*) Temperature dependence of the resistivity in n-Ge ($N = 2\times10^{17}$ cm^{-3}) subjected to compressive plastic deformations: D1, deformation-free germanium; D2, 13% deformation; D3, 25% deformation; D4, 46% deformation (see table 2). (*b*) Evolution of the resistivity of n-Ge ($N = 7\times10^{17}$ cm^{-3}) irradiated with 10^9 eV protons after isochronous anneal: P0, before irradiation; P1, immediately after; P3, $T_{ann} = 200\,^{\circ}$C; P4, $T_{ann} = 250\,^{\circ}$C; P8, $T_{ann} = 450\,^{\circ}$C; P10, $T_{ann} = 600\,^{\circ}$C.

Table 2.

	Sample No	T_{ann} (°C)	Deformation (%)	Electron concentration at 293 K (10^{17} cm^{-3})	$\sigma(T)$[a]
Plastically deformed	D2		13	1.8	$\sim\exp[-(T_0'/T)^{0.25}]$
	D3		25	1.7	$\sim\exp[-(T_0''/T)^{0.25}]$
	D4		46	1.4	$\sim T^{1.0}$
Irradiated with 10^9 eV protons	P1	Before annealing		0.45	$\sim\exp[-(T_1'/T)^{0.25}]$
	P2	150		0.96	$\sim\exp[-(T_1''/T)^{0.1}]$
	P3	200		0.86	$\sim\exp[-(T_2'/T)^{0.1}]$
	P4	250		4.8	$\sim T^{0.20}$
	P5	300		5.3	$\sim T^{0.20}$
	P7	400		5.7	$\sim T^{0.20}$
	P8	450		6.3	$\sim T^{0.20}$
	P9	500		6.3	$\sim T^{0.10}$
	P10	600		7.3	$\sim T^{0.10}$

[a] T_0', T_0'', T_1', T_1'', T_2' are constants.

Thus, after the cessation of impurity metallic conduction at relatively low deformations, when they play exclusively the role of compensating centres, the transition to the classic Mott conduction via impurities takes place. Then, when higher deformations cause formation

of an efficient conduction band, the two conduction channels coexist, viz. the remaining uncompensated donor impurities and dislocations. Their relative importance determines the type of temperature dependence of conductivity: at high deformations dislocation conduction becomes larger than impurity conduction and shunts the latter. Therefore, although upon deformation germanium remains n-type, the conductivity at $T < 30$ K shows a power-law variation with temperature down to ultra-low temperatures. Thus, under plastic deformation the MIT takes place in the system of impurities, and with increasing deformation degree (disorder) there again occurs a transition, this time from impurity (semiconductor) to dislocation (metallic) conduction. In the proton-irradiated heavily doped n-Ge far from the MIT, Mott conduction is observed. In the course of isochronous annealing of defects ($t_{ann} = 1$ h) the conductivity increases (figure 13(*b*), table 2); near the MIT the conductivity temperature dependence turns power law with subsequent return to metallic behaviour after complete annealing of radiation defects [25].

6. Electrical conductivity near the MIT of lightly doped disordered germanium produced by irradiation with high-energy neutrons and protons

Irradiation of germanium with fast reactor neutrons results in the introduction into the forbidden gap of shallow acceptor levels $E_v + 0.016$ eV [26], their depth decreasing with increasing concentration of centres (in analogy with centres due to impurities). By increasing the concentration of these centres, the low-temperature conductivity can be gradually increased to become metallic. Because this shallow centre is not an impurity but a structural defect, by appropriate thermal treatment a smooth reverse transition from metallic to insulating can be effected in the same sample. The interaction cross section of high-energy neutrons with germanium being small, of the order of a few millibarns, the uniformity of the distribution of the $E_v + 0.016$ eV centres formed happens to be higher than the impurity distribution in doped semiconductors, exceeding even the possibilities of available metrological methods. So, in contrast to impurity-doped semiconductors, on which the MIT can be studied only using a set of several samples with different impurity concentrations near the transition and poor uniformity, germanium with structural defects introduced by irradiation with high fluxes of high-energy nucleons allows study of the MIT in the same sample. The n-Ge samples ($N(\mathrm{Sb}) = 3 \times 10^{13}$ cm^{-3}) are placed in cadmium containers having 0.5 mm thick walls and are irradiated in the active zone of a VVRM water–water research reactor with an integrated flux of 10^5 eV neutrons (from 10^{18} to 3×10^{19} neutrons cm^{-2}) and of 10^9 eV protons (2×10^{17} protons cm^{-2}).

Figure 14 gives the dependence of the hole concentration in germanium at 293 K (curve a) on the integrated flux (IF) of fast neutrons. With increasing IF value the hole concentration nearly reaches saturation (a Hall factor of unity is assumed). The low-temperature conductivity in the same samples (curve b) shows a maximum. In figure 15(*a*) are seen typical temperature dependences of the conductivity and, derived from these using a Coulomb gap model [27], the variation of the Coulomb gap with parameter κa, κ being the dielectric constant and a the Bohr radius. Figure 15(*b*) shows the measured temperature variation of the hole concentration; the parameters of the low-temperature conductivity and the hole concentrations derived are given in table 3 together with isochronous anneal temperatures and integrated fluxes. The experimental data obtained show that for relatively low IF of 10^5 eV neutrons, when the total volume of a crystal occupied by disordered regions (DRs) is small, the probability of energy release in this volume on repeated interactions with fast neutrons would also be small. Therefore, the concentration of shallow acceptor centres

introduced rises practically linearly in this range of IF values. For large fluxes of fast neutrons the concentration of holes due to radiation defects saturates, and with further increase of IF the low-temperature conductivity decreases somewhat. The maximum in the low-temperature conductivity corresponds to a situation when DRs occupy a considerable part of the crystal volume and the energy production there by fast neutrons causes some ordering of atoms or recrystallization of DRs. So, at a certain IF magnitude an equilibrium is reached between the processes of defect formation and recrystallization, whereupon the defect concentration is stabilized, corresponding to the maximum low-temperature conductivity. It should be noted that the Bohr radius of a hole localized on a shallow acceptor centre produced by fast neutrons equals $a = 40$ Å [26]. In accordance with the Mott criterion, applicable to a wide range of materials, $n_c^{1/3}a = 0.25$ [28]. This corresponds to a critical concentration for the MIT of $n_c = 2.4 \times 10^{17}$ cm^{-3}. Meanwhile, as seen from experimental data in figure 15, significant weakening of the temperature dependence of the conductivity and the transition to metallic conductivity take place at an unexpectedly high hole concentration value of 1.3×10^{18} cm^{-3}, suggesting clustering of radiation defects at high concentrations. It is an increase of the distance between the acceptor centres brought about by a spatial correlation of the radiation defects that causes an effective increase of the critical concentration for the MIT.

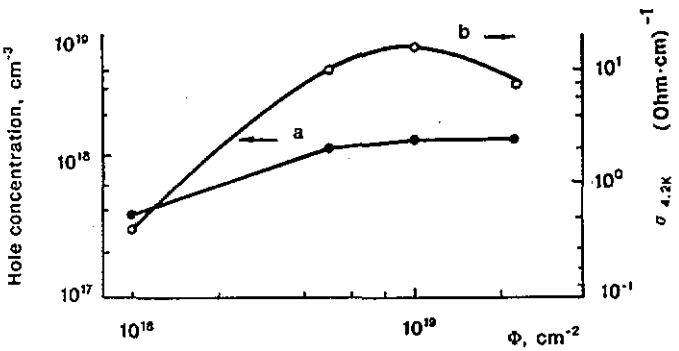

Figure 14. Hole concentration (curve a) and low-temperature electrical conductivity (curve b) of lightly doped germanium as a function of the fluence of reactor neutrons of energy $E = 10^5$ eV.

In germanium irradiated with high-energy neutrons and protons, the temperature dependence of the conductivity at low temperatures near the MIT on the insulator side follows the relationship $\rho(T) = \rho_0 \exp[(T_0/T)^{1/2}]$ (figure 15). According to the assumption of the existence of a Coulomb gap in the density of states at the Fermi level [27], $T_0 = \beta e^2/k\kappa a$. The Coulomb gap is calculated using the expression $\Delta = 0.5k(T_0T^*)^{1/2}$, where T^* is the maximum temperature at which deviation from the $T^{1/2}$ law starts. In the insert in figure 15(a) is given the dependence of the Coulomb gap Δ on the parameter κa derived from data on the temperature variation of the conductivity measured on samples irradiated with different fluences and annealed at various temperatures (see table 3). With increasing parameter κa the Coulomb gap is seen to shrink. Near the MIT the conductivity due to radiation defects, as with dislocations, shows a power-law variation with temperature, $\sigma(T) \sim T^x$, where x is less than unity and falls as the MIT is approached. That is, the power-law behaviour of the conductivity would be observed in a semiconductor irrespective of the nature of localization centres, their charge state and dimensions.

Table 1.

Fluence (10^{18} cm^{-2})	Sample No	T_{ann} (°C)	Hole concentration at 293 K (10^{17} cm^{-3})	$\sigma(T)$ (Ω^{-1} cm^{-1})[a]	Δ (10^{-3} eV)	κa (10^{-4} cm)	T (K)	T (K)
1.0	2	150	3.3	$\sim\exp[-(T_1/T)^{0.5}]$	0.69	1.37	34.2	7.5
	3	200	3.8	$\sim\exp[-(T_2/T)^{0.5}]$	0.87	1.14	13.9	10.0
	5	300	2.7	$\sim\exp[-(T_3/T)^{0.5}]$	1.16	0.55	84.9	8.5
	6	450	7.2	$\sim\exp(-E_3/kT)$; $E_3 = 5.5 \times 10^{-4}$ eV				
5.0	7	Before annealing	11	$(0.5 + 9.0T^{0.1})$				
	8	150	14	$\sim 6.2T^{0.2}$				
	9	200	11	$\sim 6.0T^{0.2}$				
	10	250	9.6	$\sim 5.6T^{0.2}$				
	11	300	6.9	$\sim\exp[-(T_4/T)^{0.5}]$	0.64	3.55	13.2	16.7
	12	350	3.0	$\sim\exp[-(T_5/T)^{0.5}]$	1.13	0.68	68.7	10.0
	29	450	0.61	$\sim\exp[-(E_3/kT)]$; $E_3 = 3.1 \times 10^{-4}$ eV				
10	13	Before annealing	13	$(3.8 + 10.5T^{0.1})$				
	14	150	13	$(0.2 + 11.4T^{0.1})$				
	15	200	13	$(0.2 + 7.8T^{0.1})$				
	16	250	14	$(0.8 + 9.2T^{0.1})$				
	17	350	4.3	$\sigma(T) = \sigma_2\exp(-E_2/kT) + \sigma_3\exp[-(T_6/T)^{0.5}]$; $E_2 = 3.6 \times 10^{-4}$ eV				
	18	450	1.3	$\sigma(T) = \sigma_3\exp(-E_3/kT)$; $E_3 \approx 10^{-4}$ eV				
30	19	Before annealing	13	$\sim 6.7T^{0.1}$				
	20	150	12	$(0.8 + 9.8T^{0.1})$				
	21	200	12	$(0.6 + 12.6T^{0.1})$				
	22	250	13	$(1.7 + 9.4T^{0.1})$				
	24	450	3.7	$\sigma(T) = \sigma_3\exp(-E_3/kT)$; $E_3 < 10^{-4}$ eV				
0.2 protons cm^{-2}	1′	Before annealing	0.29	$\sim\exp[-(T_7/T)^{0.5}]$	1.49	0.55	84.9	14.0

[a] T_1, T_2, T_3, T_4, T_5, T_6, T_7 are constants.

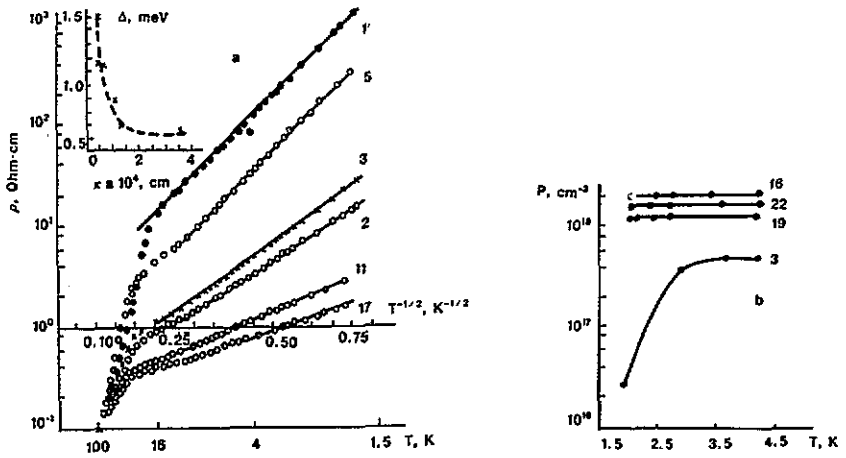

Figure 15. Temperature dependences of (*a*) electrical conductivity of germanium irradiated with reactor neutrons (samples 2, 3, 5, 11, 17) and with 10^5 eV reactor protons (sample 1′) and the calculated Coulomb gap Δ versus parameter κa for samples 1, 2, 3, 5, 11, 12; and (*b*) hole concentrations for germanium samples 3, 16, 19, 22. Sample characteristics are given in table 3.

7. Magnetoresistance of plastically deformed germanium

For structurally disordered semiconductors whose low-temperature conductivity is governed by dislocations, the problem of electrical conduction in a magnetic field has not been investigated. It is obvious that in this material, compared with impurity-doped semiconductors, additional complications arise related to the spatial extension of the defect centre, lack of information on the effect of its charge state on carrier transport, the exact form of the carrier wavefunctions and so on. At the same time research on low-temperature magnetoresistivity (MR) in PDG is of considerable importance because of the possibility to control the strength of carrier localization on dislocations or impurities (in the presence of dislocations) by controlling disorder, thus making feasible an experimental examination of the role of the localized magnetic moment in the low-temperature MR.

7.1. Lightly doped PDG

From the dependences of the transverse ($H \perp j$) and longitudinal ($H \| j$) MR given in figure 16, it is seen that on lowering the temperature the maximum in MR increases in magnitude and shifts to weaker fields. Figure 17 shows the longitudinal and transverse MR of lightly doped PDG with $D = 43\%$ at 4.2 and 2.5 K and the transverse MR for PDG with $D = 30\%$ at 4.2 K. The transverse and longitudinal MR in all samples behaves in a similar manner and has essentially the same value. With increasing deformation MR changes differently in different samples: in PDG with $D = 20\%$ a negative MR is observed for small H, followed by the usual quadratic positive MR [27] in the range $H \geqslant 50$ kOe; while for PDG with $D = 30$ and 43% an anomalous positive MR is observed that is nearly linear starting from low values of the magnetic field. From the experimental data obtained, it follows that MR in PDG as a function of magnetic field strength and temperature behaves in the same manner as in impurity-doped semiconductor materials. It is natural to suppose that the underlying physical mechanisms in both cases are identical.

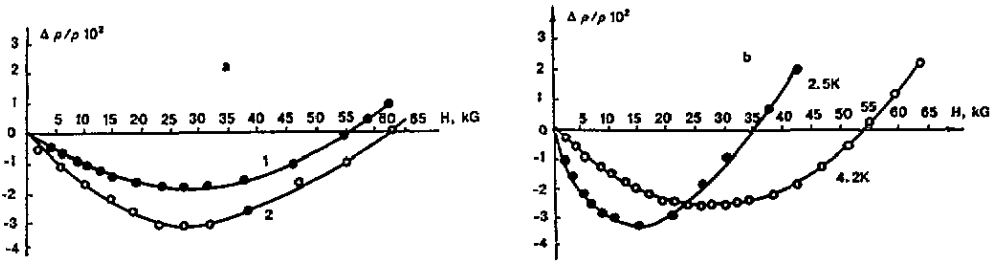

Figure 16. (*a*) Transverse ($j \perp H$) (1) and longitudinal ($j \| H$) (2) magnetoresistance of lightly doped PDG at deformation $D = 20\%$ and $T = 4.2$ K. (*b*) Transverse magnetoresistance of lightly doped PDG at deformation $D = 23\%$, $T = 4.2$ and 2.5 K.

If it is postulated that the major cause of the negative MR in PDG is the weakening by the magnetic field of carrier scattering on localized magnetic moments, then the MR for all crystallographic directions should be negative. On the other hand, because in lightly doped PDG dislocations are arranged in layers oriented predominantly in the (1 1 1) planes, a situation can arise where in the [1 1 1] direction the conductivity dependence on temperature will be exponential as in a semiconductor and in the (1 1 1) plane it will be power law or metallic, thus affording the possibility of studying the role of different factors in the occurrence of the negative MR. Experimental data pertaining to such a situation are seen in figure 18, where for a sample of PDG with $D = 43\%$ we show the magnetic field dependences at 4.2 K of the longitudinal MR measured with the probing current flowing along the [1 1 1] axis and the transverse MR for the probing current in the (1 1 1) plane: for $H \perp j$ the magnetoresistance in low fields has a positive sign, whereas for the current direction along the [1 1 1] axis ($H \| j$) negative MR is observed.

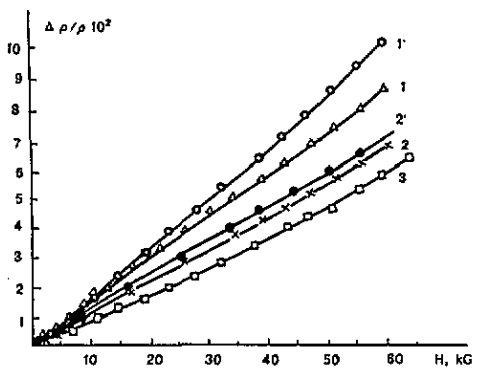

Figure 17. Magnetoresistance of lightly doped PDG: 1, 1′, transverse magneotresistance at $T = 4.2$ and 2.5 K, and 2, 2′, longitudinal magnetoresistance at $T = 4.2$ and 2.5 K, respectively, at $D = 43\%$; 3, transverse magnetoresistance at $T = 4.2$ K, at $D = 30\%$.

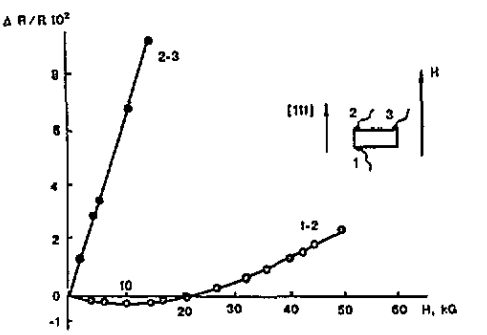

Figure 18. Magnetoresistance of PDG for $D = 43\%$ and $T = 4.2$ K in different crystallographic directions. Schematics of the experiment are given in the insert.

In effect, both positive and negative MR have been found to occur in the same sample in different crystallographic directions! If the inhibition of carrier scattering by a magnetic field

were the main cause of the negative MR, then it would have been observed in the (1 1 1) plane as well, since in this plane the electrical conductivity has metallic character, with carriers free to move, so no reasons exist to suppose the absence of scattering by localized magnetic moments. A conclusion to be drawn from this experiment is that the carrier transport mechanism is responsible for the negative MR observed, not carrier scattering by localized magnetic moments. This conclusion is supported by the observation that the negative MR invariably appears in PDG when the hopping (exponential) conduction proceeds via dislocations (whereas for the power-law temperature dependence of conductivity on the metallic side of the MIT the anomalous positive MR is observed).

7.2. Doped disordered germanium

In figures 19–21 are given the magnetic field dependences of the transverse MR for germanium with different deformations and initial impurity concentrations (Sb and Ga), measured with the current flowing in the (1 1 1) plane. In n-Ge with impurity concentration $N = 2.5 \times 10^{16}$ cm^{-3} the MR varies in the usual way for semiconductors with 'E_3 conduction': in low fields with increasing deformation the MR turns negative and with further increase in deformation (upon transition to conduction via dislocations) becomes sublinear, as in intrinsic Ge with $D = 43\%$. For n-Ge with $N = 4.9 \times 10^{17}$ cm^{-3} (figure 20) the negative MR is observed in low fields, as in the non-deformed starting samples, but of smaller magnitude. In high fields the MR turns positive and quadratic in field strength. In p-Ge with $N = 8 \times 10^{15}$ cm^{-3} (figure 21) deformation causes negative MR in low magnetic fields and with increasing field the MR again turns positive and quadratic in field strength. Though the conductivity of p-Ge at liquid-helium temperatures remains unchanged up to 33% deformation, as seen in figure 9, in low fields the negative MR can be induced by introducing large amounts of dislocations.

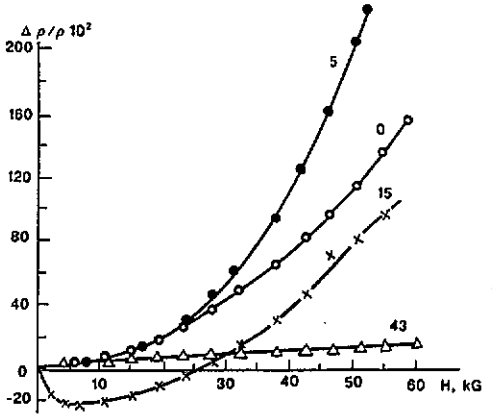

Figure 19. Transverse magnetoresistance of PDG with initial impurity concentration $N = 3 \times 10^{13}$ cm^{-3} at $T = 4.2$ K. Figures by the curves give plastic deformation values ($j \perp [1\,1\,1]$).

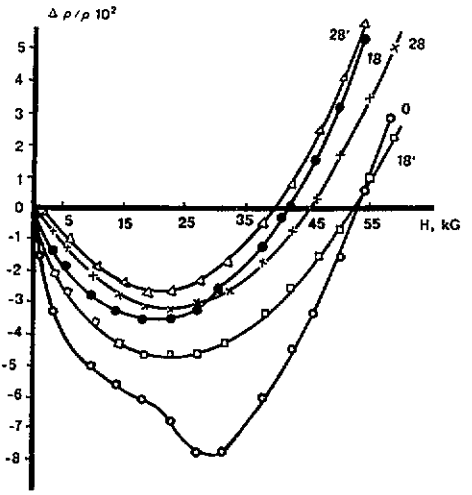

Figure 20. Transverse magnetoresistance of PDG with initial impurity concentration $N = 4.9 \times 10^{17}$ cm^{-3} at $T = 4.2$ K. Figures by the curves give plastic deformation values for $j \perp [1\,1\,1]$ and primed figures for $j \parallel [1\,1\,1]$. Curve 0 is the starting sample subjected to a standard thermal treatment but not plastically deformed.

7.3. On dislocation conduction in silicon

The experimental data obtained show that at low temperatures transport phenomena in germanium with structural disorder produced by extended defects exhibit a number of features. Are these features an exclusive property of germanium or have they a more general character? In particular, is it possible that conductivity via dislocations (or in the defect band) exists in other materials, e.g. silicon, which has a similar structure? For example, dislocations are known to affect considerably galvanomagnetic phenomena in plastically deformed Si [29]. In a conductivity study [30] of plastically deformed silicon (PDS) with initial impurity (phosphorus) concentration $N = 5 \times 10^{16}$ cm^{-3}, anomalies in the HP were observed at liquid-helium temperatures for deformations $D \leqslant 6\%$ caused, allegedly, by formation of an additional conduction channel via dislocations. In view of the small magnitude of the observed anomalies, this suggestion is questionable, leaving the possibility of other factors, e.g. thermal treatment or electrical fields due to dislocations, being involved. To throw more light on this problem, at least concerning the two semiconductors with the diamond structure, germanium and silicon, experiments were undertaken, which we describe below.

As a starting material n-Si with a phosphorus concentration $N = 5 \times 10^{13}$ cm^{-3} was chosen, which at $T = 4.2$ K is an insulator with conductivity, if any, governed by the dislocations introduced. Wafers of n-Si having a thickness of 3 mm were subjected to compressive strain along the [1 1 1] axis in air at 1000 °C using a W–Re punch, producing deformations of up to 70%, and, after cooling at a rate slower than 10 °C min^{-1}, lapped ($\approx 20\mu$m off each face) and etched in a mixture of nitric and hydrofluoric acids. After this treatment all samples were found to be p-type. Ohmic contacts were prepared using a technique involving low-temperature solid-phase epitaxy of Al developed earlier [31] for high-resistivity p-Si ($\rho \approx 10^4$ Ω cm) for use in nuclear detectors. Aluminium is deposited by evaporation in a vacuum of $p < 10^{-5}$ Torr onto an Si wafer heated to 450 °C, and after cooling the wafer at a rate not exceeding 5 °C min^{-1} its surface is electroplated with Ni. The current–voltage characteristic of this contact at temperatures of 77 and 300 K can be seen in [31]. The silicon samples with $D = 30$ and 70% have room-temperature resistivities of 1.8×10^5 and 2.2×10^5 Ω cm, respectively, and an exponential temperature dependence of the resistivity with an activation energy close to $E_g/2$ or about 0.5 eV in both samples. Therefore, when even slightly cooled, PDS samples exhibit large resistivities and at $T = 77$ K become insulating with $\rho > 10^{12}$ Ω cm, because conduction due to dislocations is absent. All the above comments refer also to Si irradiated with fast ($E = 0.1$ MeV) neutrons at integrated fluxes up to 10^{19} neutrons cm^{-2}. Plastic deformation affects the properties of Ge and Si in essentially the same way as irradiation with highly energetic elementary particles. With increasing fluence of fast neutrons or protons, the Fermi level in Ge shifts towards the valence band and in Si it gets pinned at mid-gap. Seemingly, this behaviour corresponds to the crystal-defect system tending to a minimum in free energy [32].

7.4. On the structure of plastically deformed germanium

Characteristic features of dislocation conduction in PDG are very reminiscent of impurity conduction features: with increasing magnitude of plastic deformation D the ionization energy E of levels due to dislocations lowers, the low-temperature conductivity by hopping of carriers localized at dislocations rises exponentially (unless D does not exceed 30%), and the MIT observed. These analogies in electrical behaviour entitle one to speak of 'dislocation doping' of single-crystal germanium. A question arises, however, as to what degree the crystalline structure of germanium is affected by high densities of dislocations.

Neutron diffractometry studies of the crystal structure of germanium subjected to plastic deformation are carried out with a three-crystal spectrometer placed in the horizontal channel of a VVRM research reactor. The measuring technique has been described elsewhere [4]. Rocking curves shown in figure 22 are measured for 1 1 1 reflection in specimens with different D values. It is seen that, with increasing D, the half-width of the rocking curves increases and the reflection coefficient of slow neutrons in the curve maximum drops. This behaviour is usual for 'mosaic' crystals when disorientation of the crystal blocks increases. At the same time, in PDG up to $D = 23\%$ the misorientation angle does not exceed 4%. The x-ray diffractogram for PDG with $D = 0.8\%$ obtained using the Berg–Barret technique [33] gives a picture of high dislocation density, small misorientation angles and considerable residual microstrain. Still, the corresponding x-ray diffractogram has the appearance typical of a single crystal, which is supported by neutron diffraction data, whereas in the diffractogram for PDG with $D = 23\%$, instead of point reflections, a smeared arc is observed typical for textured polycrystals. For PDG with $D = 43\%$ the diffractogram consists of concentric circles, as in polycrystals. So, the structure of PDG changes with increasing deformation from monocrystalline to mosaic followed by textured polycrystalline and, ultimately, polycrystalline.

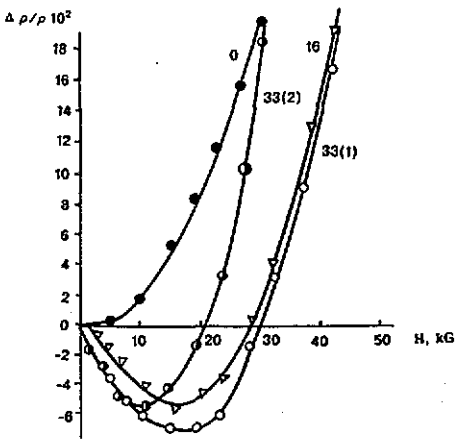

Figure 21. Transverse magnetoresistance [1 1 1] $\perp j \perp H$ at 4.2 K for PDG with initial concentration $N = 8 \times 10^{15}$ cm^{-3}. Figures by the curves give plastic deformation values. For sample $D = 33\%$, curve 33(2) is the magnetoresistance at $T = 3.4$ K.

8. On modelling of physical phenomena in amorphous semiconductors

Numerous processes in amorphous and vitreous semiconductors proceed in a peculiar manner, differing considerably from crystalline semiconductors [19]. Some phenomena observed in amorphous semiconductors, in particular those related to the presence of a high density of localized states and irregular potential profile, can be modelled using analogies with heavily doped and compensated (HDC) single-crystal semiconductors [34]. A random distribution of charged impurities causes fluctuations of the potential seen by the charge carriers and leads to distortions of the boundaries of the energy bands. The distribution and extent of these fluctuations can be controlled by changing concentrations and ratios of the main and compensating impurities. It is obvious also that not all the phenomena occurring in different types of amorphous semiconductor can be simulated

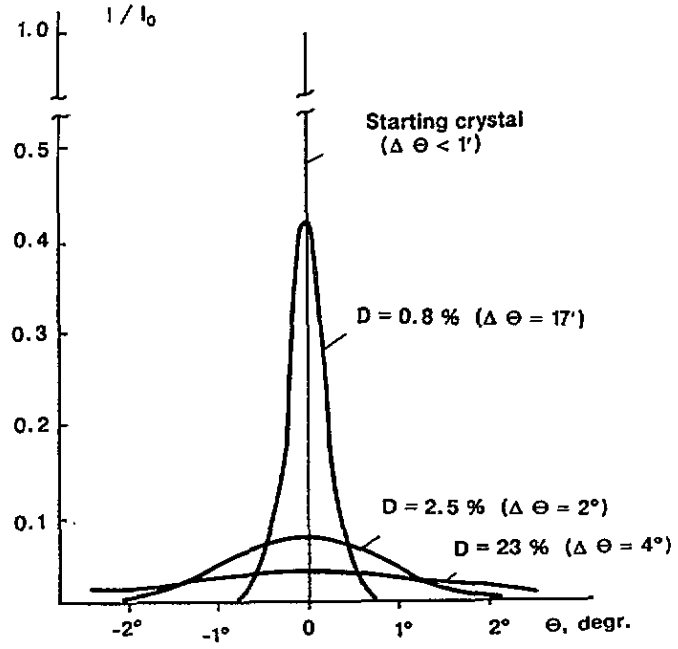

Figure 22. Rocking curves for the (1 1 1) reflection. The wavelength of neutrons $\lambda = 1.52$ Å.

with HDC semiconductors. Structural disordering is one example, because even heavily doped semiconductors remain perfectly monocrystalline. In this aspect crystals with a high density of extended defects offer additional possibilities for modelling of non-crystalline semiconductors. Indeed, on the one hand, dislocations introduce localized states within the band gap and, having been screened with a positive charge around them formed after the capture of electrons, as happens in Ge, give rise to chaotic potential relief analogous to that in HDC semiconductors. On the other hand, in diamond-like semiconductors (Ge, Si) atoms on edge dislocations located at the boundary of semiplanes have dangling bonds, seemingly the most common defect in non-crystalline semiconductors. Therefore, highly plastically deformed crystalline semiconductors, along with HDC semiconductors, can be considered as a model of amorphous semiconductors. Their properties can be controlled by varying deformation value, crystallographic direction in which it is applied and concentration of chemical impurities in the starting crystal. It should be taken into account, however, that, in contrast to chemical impurities, dislocations represent extended defects and are anisotropically distributed, which affects the transport phenomena in highly deformed crystals in a peculiar way. Consider some effects observed on passing current through structurally disordered crystalline and amorphous semiconductors and compare the temperature dependences of resistivity for amorphous germanium (a-Ge) prepared by vacuum deposition (figure 23 [35]) with the curves for lightly and moderately doped PDG (plotted on the same scale) in figures 4, 7 and 8, respectively.

It can be seen that in PDG deformed to various degrees the same type of conductivity variation with temperature as in a-Ge can be observed: conductivity with a constant activation energy E, conductivity with variable activation energy and metallic conductivity. It is clear that by varying the conditions under which a-Ge is produced (here, the substrate

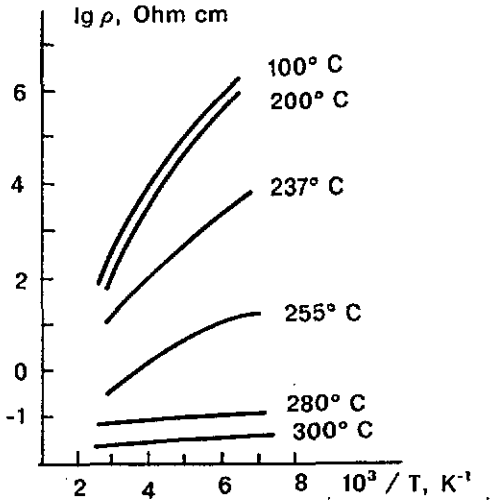

Figure 23. Temperature dependences of the resistivity for a-Ge samples [35] prepared at different substrate temperatures (figures by the curves) during deposition.

temperature during deposition) or the degree of deformation of PDG, the number of dangling bonds, which determines the type of conductivity, can be controlled. Formation of a quasi-continuous spectrum of localized states in the band gap makes the activation energy of conductivity decrease continuously on lowering the temperature and, ultimately, Mott-type conductivity is obtained. Typically, current–voltage characteristics (CVCs) of amorphous semiconductors are superlinear and their non-linearity increases with decreasing temperature; in strong electric fields they become temperature independent [36]. Shown in figure 24 are CVCs for a-Ge [36] and lightly doped PDG samples with $D = 20$ and 30% at low temperatures. The above-mentioned features of CVCs in amorphous semiconductors are seen to be exhibited also by PDG, the important parameter being the number of dangling bonds (determined by preparation conditions of a-Ge and deformation value). For various values of this parameter in lightly doped PDG the negative transverse MR can be observed in low magnetic fields, influenced weakly by the angle between current and field directions, a picture similar to what is observed in amorphous semiconductors a-Ge and a-Si [37–39].

Consider optical absorption in disordered PDG shown in figure 25 [40]. In both a-Ge and a-Si [19], with increasing D the fundamental absorption edge in PDG shifts to longer wavelengths and broadens, and a structureless band appears at < 0.25 eV, while absorption bands in the range 0.25–0.6 eV are absent. The shift and broadening are caused by two factors: (i) electron transitions from the acceptor-type dislocation band to the conduction band; and (ii) interband absorption variation caused by disorder, i.e. by band positions being affected by the chaotic potential due to dislocations, which has electrostatic and deformation components. A similar though much weaker shift of the absorption edge with increasing degree of compensation is found in HDC germanium. In this case the material remains structurally perfect, the chaotic potential being produced by electrical charges of randomly distributed donors and acceptors. This kind of potential distorts both conduction and valence bands in a similar way ('in phase'); therefore the band-gap value stays the same everywhere, while the long-wavelength shift is due to electron transitions with simultaneous tunnelling. The deformation component of the chaotic potential relief in PDG produces an 'out-of-phase' distortion of the band edges, by causing density fluctuations or changing the work function on the microcrystalline faces [41]. Therefore, the band edge shift is not necessarily accompanied by tunnelling of carriers, which explains the large magnitude of the effect, of the same order as in amorphous Ge and Si. The data presented show that

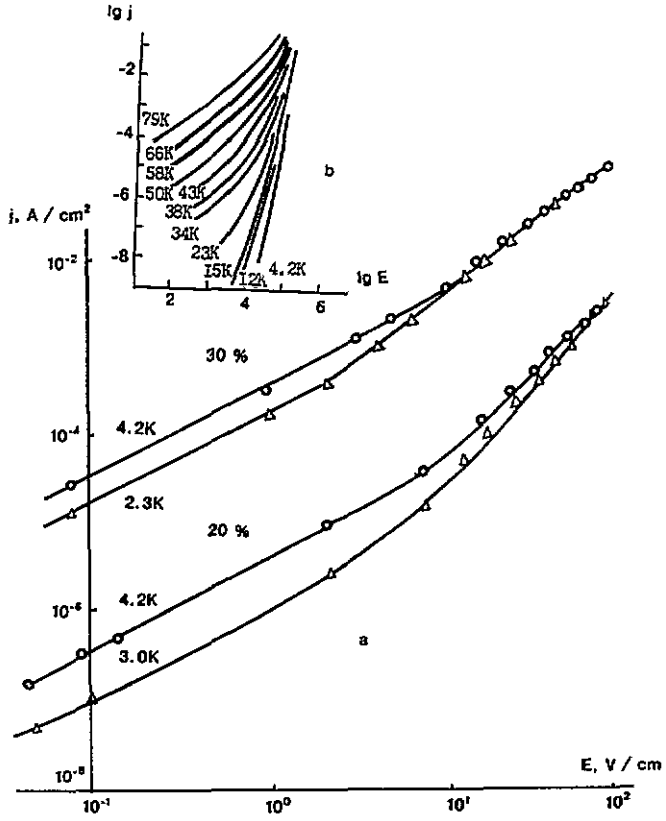

Figure 24. Current–voltage characteristics for (*a*) lightly doped plastically deformed (20 and 30%) germanium at liquid-helium temperatures and (*b*) a-Ge [36].

physical phenomena in a-Ge can indeed be modelled using both HDC semiconductors and PDG. In other amorphous semiconductors, for example a-Si, the situation is totally different. The dangling bonds appearing in a-Si produced using different techniques introduce a high density of localized states in the conduction band, while the electrical conductivity is essentially intrinsic and weakly varying, one exception being hydrogenated silicon Si(H), where bonds are saturated with hydrogen. Therefore a-Si cannot be simulated with HDC semiconductors doped with shallow impurities. Plastically deformed Si (PDS) can serve as a model for studying a-Si, because in PDS the number of dangling bonds is related to the degree of deformation in the same way as it is to the substrate temperature during deposition of a-Si, and the electrical conductivity is unaffected by deformation. Above a certain value of the density of dangling bonds (deformation value) in a-Si and PDS, the Fermi level gets pinned in a position close to the mid-gap. The experimental data presented show that highly plastically deformed crystalline Ge and Si can be used for simulating some physical phenomena in amorphous semiconductors.

9. Conclusions

Investigations of low-temperature carrier transport in disordered germanium have revealed basic laws governing the electrical conductivity in the defect band, formed due to the

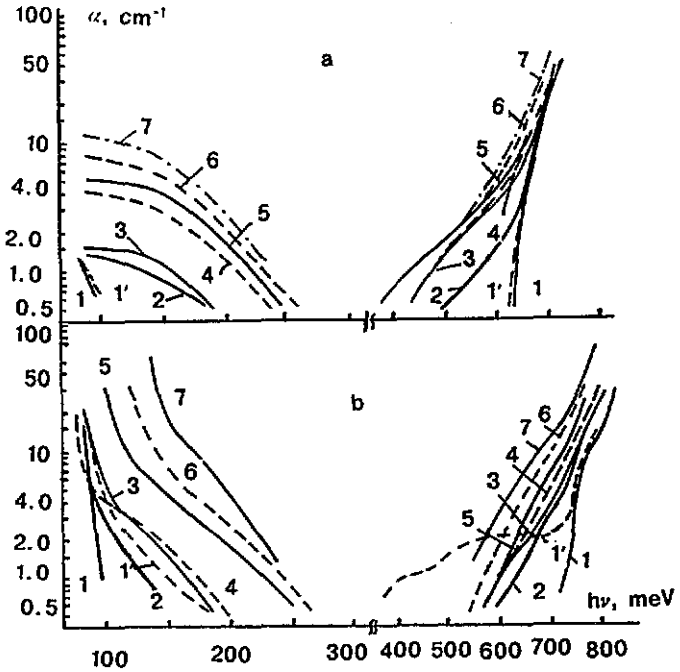

Figure 25. Optical absorption spectra of lightly doped germanium as a function of deformation value at (*a*) 300 and (*b*) 77 K: 1, initial; 1′, reference sample after thermal treatment; 2, $D = 9\%$; 3, $D = 12\%$; 4, $D = 14\%$; 5, $D = 20\%$; 6, $D = 30\%$; 7, $D = 40\%$.

presence of large concentrations of extended defects of different nature, and allowed development of models of a number of phenomena occurring in amorphous semiconductors. Controlled disorder in crystalline germanium produced by dislocation doping affords an easy means of controlling the character of variation and the value of conductivity at low and ultra-low temperatures, so a new method of producing cryogenic thermoresistors can be proposed for the temperature range in question [42]. Introduction of large quantities of extended defects for controlling the structure of crystalline germanium both during growth [43] and by producing plastic deformations allows one to obtain large mosaic crystalline monochromators of slow neutrons with high reflectivity in the peak of the rocking curve (up to 60%) and in different crystallographic orientations, (1 1 0), (1 0 0), (1 1 1) [44].

Acknowledgments

Fruitful and stimulating discussions with and the help of Drs I S Shlimak and N S Lipkina are acknowledged with much gratitude. Thanks are due also to Drs A G Gukasov, A I Kovalev, I V Klyatskina, A S Rybalko, R Rench, I L Shulpina and K N Zinovjeva for their help with experiments.

References

[1] Davis E A and Compton W D 1965 *Phys. Rev.* **140** 2183

[2] Wolf E L, Compton W D and Depp S W 1966 *J. Appl. Phys.* **37** 4941
[3] Osipjan Ju A and Shevchenko S A 1974 *Pis. Zh. Eksp. Teor. Fiz.* **20** 709 (in Russian)
[4] Zabidarov E I, Kozhukh M L, Trunov V A, Vakhrushev S B, Okuneva N M and Belokurova I N 1979 *Preprint* Leningrad Nuclear Physics Institute, AS USSR, No 458 (in Russian)
[5] Klyatskina I V, Kozhukh M L, Ryvkin S M, Trunov V A and Shlimak I S 1979 *Fiz. Tekh. Poluprov.* **13** 1089 (in Russian)
[6] Kozhukh M L and Shlimak I S 1982 *Problems of Physics of Disordered Systems. Optical Phenomena in Semiconductors (Proc. Xth Winter School on Semiconductor Physics, A F Ioffe Institute, Leningrad)* p 67 (in Russian)
[7] Fritzshe H and Cuevas M 1960 *Phys. Rev.* **119** 1238
[8] Fritzshe H 1958 *J. Phys. Chem. Solids* **6** 69
[9] Merchant P and Elbaum C 1978 *Solid State Commun.* **26** 73
[10] Fridel G 1967 *Dislocations* (Moscow: Mir) (in Russian)
[11] Mott N F and Twose W D 1961 *Adv. Phys.* **10** 107
[12] Shklovski B I and Shlimak I S 1972 *Fiz. Tekh. Poluprov.* **6** 129 (in Russian)
[13] Shklovski B I 1977 *Fiz. Tekh. Poluprov.* **11** 2135 (in Russian)
[14] Boltaks B I 1972 *Diffusion and Point Defects in Semiconductors* (Leningrad: Nauka) (in Russian)
[15] Klyatskina I V, Kozhukh M L, Ryvkin S M, Trunov V A and Shlimak I S 1979 *Pis. Zh. Eksp. Teor. Fiz.* **29** 268 (in Russian)
[16] Klyatskina I V, Kozhukh M L, Ryvkin S M, Trunov V A and Shlimak I S 1982 *Doping of Semiconductors* (Moscow: Nauka) p 236 (in Russian)
[17] Kozhukh M L, Lipkina N S and Tarkhin D V 1987 *Fiz. Tekh. Poluprov.* **27** 680 (in Russian)
[18] Erykalov A N, Ignatenko E I, Kozhukh M L, Litovchenko A V, Markov Ju V and Petrov Ju V 1988 *Atomnaja Energia* **65** 24 (in Russian)
Kozhukh M L 1993 *Nucl. Instrum. Methods* in press
[19] Mott N F and Davis E A 1979 *Electron Processes in Non-Crystalline Materials* (Oxford: Clarendon)
[20] Shlimak I S and Nikulin E P 1972 *Pis. Zh. Eksp. Teor. Fiz.* **15** 30 (in Russian)
[21] Zinov'eva K N, Kozhukh M L, Ryvkin S M, Trunov V A and Shlimak I S 1979 *Pis. Zh. Eksp. Teor. Fiz.* **30** 303 (in Russian)
[22] Ionov A N 1980 *Fiz. Tekh. Poluprov.* **14** 1287 (in Russian)
[23] Osipjan Ju A and Shevchenko S A 1981 *Pis. Zh. Eksp. Teor. Fiz.* **33** 65 (in Russian)
[24] Goncharov V A, Osipjan Ju A and Shevchenko S A 1987 *Solid State Phys.* **29** 1928 (in Russian)
[25] Kozhukh M L and Lipkina N S 1987 *Phys. Status Solidi* a **100** 259
[26] Dobrego V P, Ermolaev O P and Tkachev V D 1977 *Phys. Status Solidi* a **44** 435
[27] Shklovski B I and Efros A L 1979 *Electronic Properties of Doped Semiconductors* (Moscow: Nauka) (in Russian)
[28] Edwards P P and Sienko M Y 1978 *Phys. Rev.* **17** 2275
[29] Eremenko V G, Nikitenko V I and Jakimov E B 1977 *Zh. Eksp. Teor. Fiz.* **73** 1129 (in Russian)
[30] Grazhulis V A, Mukhina V Ju, Osipjan Ju A and Shevchenko S A 1975 *Zh. Eksp. Teor. Fiz.* **68** 2149 (in Russian)
[31] Kozhukh M L and Morozov V F 1975 *Pribory Tekh. Eksp.* **6** 241 (in Russian)
[32] Smirnov L S (ed) 1980 *Physical Processes in Irradiated Semiconductors* (Novosibirsk: Nauka) p 142 (in Russian)
[33] Kozhukh M L, Ryvkin S M, Trunov V V, Shlimak I S and Shulpina I L 1980 *Fiz. Tekh. Poluprov.* **14** 2279 (in Russian)
[34] Ryvkin S M and Shlimak I S 1973 *Phys. Status Solidi* a **16** 515
[35] Noda M, Marino S and Yamada T 1977 *Japan. J. Appl. Phys.* **11** 1119
[36] Morgan M and Walley P A 1971 *Phil. Mag.* **23** 661
[37] Mell M and Stucke J 1970 *J. Non-Cryst. Solids* **4** 307
[38] Thomas P, Barna A, Barna P B and Radnoczi G 1975 *Phys. Status Solidi* a **30** 637
[39] Clark A N, Cohen M M, Capri M and Lanyon H P 1974 *J. Non-Cryst. Solids* **16** 117
[40] Shlimak I S, Kozhukh M L, Rench R and Fridland F 1983 *Fiz. Tekh. Poluprov.* **17** 955 (in Russian)
[41] Ryvkin S M 1973 *Phys. Status Solidi* a **19** K173
[42] Kozhukh M L 1992 *Cryogenics* **32** 537
[43] Kozhukh M L, Belokurova I N, Vakhrushev S B, Shulpina I L and Titkov A N 1983 *Nucl. Instrum. Methods* **213** 483
[44] Kozhukh M L 1992 *Germanium Monochromators of Slow Neutrons (MSN), X-rays and γ-radiation* A F Ioffe Physico-Technical Institute Special Edition (St Petersburg: A F Ioffe Institute)